VOLUME 120, NUMBER 37
SEPTEMBER 23, 1998

JOURNAL OF THE AMERICAN CHEMICAL SOCIETY

Continuum Solvent Studies of the Stability of DNA, RNA, and Phosphoramidate−DNA Helices

Jayashree Srinivasan,[†] Thomas E. Cheatham, III,[‡] Piotr Cieplak,[§] Peter A. Kollman,[||] and David A. Case*,[†]

Contribution from the Department of Molecular Biology, The Scripps Research Institute, La Jolla, California 92037, Division of Computer Research and Technology, National Institutes of Health, Bethesda, Maryland 20892, Department of Chemistry, University of Warsaw, Pasteura 1, Warsaw 02-093, Poland, and Department of Pharmaceutical Chemistry, University of California, San Francisco, California 94143

Received May 27, 1998

Abstract: We apply continuum solvent models to investigate the relative stability of A- and B-form helices for three DNA sequences, d(CCAACGTTGG)$_2$, d(ACCCGCGGGT)$_2$, and d(CGCGAATTCGCG)$_2$, a phosphoramidate-modified DNA duplex, p(CGCGAATTCGCG)$_2$, in which the O3′ atom in deoxyribose is replaced with NH, and an RNA duplex, r(CCAACGUUGG)$_2$. Structures were taken as snapshots from multi-nanosecond molecular dynamics simulations computed in a consistent fashion using explicit solvent and with long-range electrostatics accounted for using the particle−mesh Ewald procedure. The electrostatic contribution to solvation energies were computed using both a finite-difference Poisson−Boltzmann (PB) model and a pairwise generalized Born model; nonelectrostatic contributions were estimated with a surface-area-dependent term. To these solvation free energies were added the mean solute internal energies (determined from a molecular mechanics potential) and estimates of the solute entropy (from a harmonic analysis). Consistent with experiment, the relative energies favor B-form helices for DNA and A-form helices for the NP-modified system and for RNA. Salt effects, modeled at the linear or nonlinear PB level, favor the A-form helices by modest amounts; for d(ACCCGCGGGT)$_2$, salt is nearly able to switch the conformational preference to "A". The results provide a physical interpretation for the origins of the relative stabilities of A- and B-helices and suggest that similar analyses might be useful in a variety of nucleic acid conformational problems.

1. Introduction

The notion that DNA helices can be found in both "A" and "B" forms, depending upon the environment, has been known for many years, preceding even the elucidation of their basic structures by diffraction methods in the 1950s. Yet it is only in recent times that solvated molecular simulation methods have been able to reproduce the (local) stability of these states. Many early molecular dynamics simulations of nucleic acid duplexes required artificial constraints to keep the strands from separating;[1] careful examination of the force fields used, along with implementation of efficient ways of handling long-range

[†] The Scripps Research Institute.
[‡] National Institutes of Health.
[§] University of Warsaw.
[||] University of California.

(1) McConnell, K. J.; Nirmala, R.; Young, M. A.; Ravishankar, G.; Beveridge, D. L. *J. Am. Chem. Soc.* **1994**, *116*, 4461−4462.
(2) Auffinger, P.; Westhof, E. *Curr. Opin. Struct. Biol.* **1998**, *8*, 227−236.
(3) Spector, T. L.; Cheatham, T. E., III; Kollman, P. A. *J. Am. Chem. Soc.* **1997**, *119*, 7095−7104.

S0002-7863(98)01844-7 CCC: $15.00
Published on Web 08/26/1998

Table 1. Results for d(CCAACGTTGG)$_2$

	"BD1"		"AD1"			
energy	mean[a]	σ[b]	mean[a]	σ[b]	(B − A)	notes
$\langle E(\text{elec})\rangle$	−88.9	3.3	204.4	5.7	−293.3	Coulomb energy
$\langle E(\text{vdW})\rangle$	−166.8	0.8	−159.1	0.9	−7.7	van der Waals energy
$\langle E(\text{int})\rangle$	860.5	1.9	867.5	1.7	−7.0	internal energy
$\langle E(\text{gas})\rangle$	604.8	3.6	912.7	5.8	−307.9	total vacuum energy
$\langle E(\text{nonpolar})\rangle$	22.8	0.0	22.6	0.0	0.2	nonpolar solvation energy
$\langle E(\text{PB})\rangle$	−4833.5	2.9	−5120.1	5.4	286.6	Poisson Boltzmann
$\langle E(\text{GB})\rangle$	−4838.0	2.9	−5126.1	5.5	288.1	generalized Born
$\langle E(\text{elec\_tot})\rangle$	−4922.3	0.9	−4915.8	1.0	−6.5	$E(\text{elec}) + E(\text{PB})$
$\langle E(\text{tot})\rangle$	−4205.8	1.8	−4184.8	1.6	−21.0	$E(\text{gas}) + E(\text{PB}) + E(\text{nonpolar})$
⟨salt: 0.1 M⟩	−28.9	0.0	−30.1	0.0	1.2	linear salt contribution
⟨salt: 0.1 M⟩	−31.9	0.0	−37.1	0.1	5.2	nonlinear salt contribution
⟨salt: 1.0 M⟩	−39.9	0.0	−45.9	0.1	6.0	nonlinear salt contribution

[a] Average energies from 100 structures, in kcal/mol. [b] Standard errors of the mean energies.

electrostatic interactions, have now made it possible to carry out stable simulations of B-form DNA for many nanoseconds and to show that the same average structure is obtained for a variety of starting configurations, including A-form helices;[2−8] although it can still be difficult to obtain truly equilibrated explicit solvent simulations.[9] It has also been possible to show that DNA can be shifted toward the A-form by adding alcohol or cobalt hexaammine ions to the computational environment in a way that closely mimics what is seen experimentally.[10,11] Modifications of the nucleic acid backbone are also of considerable interest, and we consider here a phosphoramidate system, with O3′ of the deoxy sugar replaced with NH, which has been shown in both experiment and computation to favor A-form helices in water.[12] Similarly, simulations of RNA A-form helices are stable in water, and B helices will convert spontaneously to A, but only when special techniques are used to artificially lower the barriers between these forms.[5]

The general successes of these explicit simulations open new possibilities for examining two questions. First, we use continuum solvent and surface area models to ask: what is the origin of the relative stabilities of A- and B-helices? Second, what is the salt dependence of the A−B transition for various sequences? Our approach allows the calculation of the conformational free energy differences between A- and B-helices without the need to establish an explicit sampling pathway connecting one form of helix to the other, such as by using umbrella potentials along a particular reaction pathway.[13] Such a calculation would be feasible but computationally demanding for such a large conformational change. The estimate for the relative free energy of A-RNA and B-RNA is particularly important since, unlike the corresponding DNA helices, these do not spontaneously interconvert during nanosecond simulations.[4]

The basic approach used here follows one that we and others have used for some time to analyze peptide and protein conformations.[14−20] Solute configurations are sampled as "snapshots" from a molecular dynamics simulation using explicit solvent. For each solute configuration, the "gas-phase" energy is estimated using the same molecular mechanics potential that was used to perform the simulation, but all solvent molecules are ignored, and no cutoffs are used in evaluating the nonbonded interactions. Free energies of solvation are then reintroduced by using a numerical Poisson−Boltzmann calculation for the electrostatic portion and a surface-area-dependent term for nonelectrostatic contributions to solvation.[21] Solute entropy contributions are estimated from a harmonic analysis. Details are given in the Methods.

2. Results

Our basic results are summarized in Tables 1−5. The total free energy estimates, labeled $\langle E(\text{tot})\rangle$, favor B-form helices for the three DNA sequences and A-form helices for RNA and the phosphoramidate-modified DNA, in agreement with experiment. In each case, the means are given for 100 snapshots, and σ is the standard error in the mean, which for 100 points is roughly one-tenth the sample standard deviation. For this number of snapshots, the statistical uncertainty in energy difference between A- and B-helices is less than 2 kcal/mol. In the following paragraphs we analyze these energy differences to provide a semiquantitative picture of the origins of these helical preferences.

2.1. Electrostatic Interactions. One of the principal differences between A- and B-form helices lies in the phosphate−phosphate repulsions, which are greater in the A-form, where

(4) Cheatham, T. E., III; Kollman, P. A. *J. Am. Chem. Soc.* **1997**, *119*, 4805−4825.
(5) Cheatham, T. E., III; Miller, J. L.; Spector, T. I.; Cieplak, P.; Kollman, P. A. In *Molecular Modeling of Nucleic Acids*; Leontis, N. B., SantaLucia, J., Eds.; American Chemical Society, Washington, DC, 1998; pp 285−303.
(6) Young, M. A.; Ravishanker, G.; Beveridge, D. L. *Biophys. J.* **1997**, *73*, 2313.
(7) Beveridge, D. L.; Young, M. A.; Sprous, D. In *Molecular Modeling of Nucleic Acids*; Leontis, N. B., SantaLucia, J., Eds.; American Chemical Society: Washington, DC, 1998; pp 260−284.
(8) MacKerell, A. D., Jr. In *Molecular Modeling of Nucleic Acids*; Leontis, N. B., SantaLucia, J., Eds.; American Chemical Society: Washington, DC, 1998; pp 304−311.
(9) Feig, M.; Pettitt, B. M. *J. Phys. Chem. B* **1997**, *101*, 7361−7363.
(10) Cheatham, T. E., III; Kollman, P. A. *Structure* **1997**, *5*, 1297−1311.
(11) Sprous, D.; Young, M. A.; Beveridge, D. L. *J. Phys. Chem. B* **1998**, *102*, 4658.
(12) Cieplak, P.; Cheatham, T. E., III; Kollman, P. A. *J. Am. Chem. Soc.* **1997**, *119*, 6722−6730.
(13) Valleau, J. P.; Torrie, G. M. In *Modern Theoretical Chemistry, Vol. 5: Statistical Mechanics, Part A, Equilibrium Techniques*; Berne, B. J., Ed.; Plenum Press: New York, 1977.
(14) Ösapay, K.; Young, W.; Bashford, D.; Brooks, C. L., III; Case, D. A. *J. Phys. Chem.* **1996**, *100*, 2698−2705.
(15) Bashford, D.; Case, D. A.; Choi, C.; Gippert, G. P. *J. Am. Chem. Soc.* **1997**, *119*, 4964−4971.
(16) Demchuk, E.; Bashford, D.; Gippert, G.; Case, D. A. *J. Mol. Biol.* **1997**, *270*, 305−317.
(17) Yang, A.-S.; Honig, B. *J. Mol. Biol.* **1995**, *252*, 351−365.
(18) Yang, A.-S.; Honig, B. *J. Mol. Biol.* **1995**, *252*, 366−376.
(19) Yang, A.-S.; Hitz, B.; Honig, B. *J. Mol. Biol.* **1996**, *259*, 873−882.
(20) Smith, K. C.; Honig, B. *Proteins* 1994, 18, 119−132.
(21) Honig, B.; Sharp, K.; Yang, A.-S. *J. Phys. Chem.* **1993**, *97*, 1101−1109.
(22) Cornell, W. D.; Cieplak, P.; Bayly, C. I.; Gould, I. R.; Merz, K. M., Jr.; Ferguson, D. M.; Spellmeyer, D. C.; Fox, T.; Caldwell, J. W.; Kollman, P. A. *J. Am. Chem. Soc.* **1995**, *117*, 5179−5197.

Table 2. Results for d(ACCCGCGGGT)$_2$

	"BD2"		"AD2"			
energy	mean[a]	σ[b]	mean[a]	σ[b]	(B − A)	notes
⟨*E*(elec)⟩	−470.6	3.1	−256.4	9.2	−214.2	Coulomb energy
⟨*E*(vdW)⟩	−166.6	0.9	−164.2	0.9	−2.4	van der Waals energy
⟨*E*(int)⟩	862.2	1.8	864.9	1.9	−2.7	internal energy
⟨*E*(gas)⟩	225.0	3.3	444.4	9.5	−219.4	total vacuum energy
⟨*E*(nonpolar)⟩	22.8	0.0	22.6	0.0	0.2	nonpolar solvation energy
⟨*E*(PB)⟩	−4808.8	2.8	−5018.2	8.6	209.4	Poisson Boltzmann
⟨*E*(GB)⟩	−4807.8	2.8	−5015.1	8.7	207.3	generalized Born
⟨*E*(elec_tot)⟩	−5279.4	1.0	−5274.6	1.0	−4.8	*E*(elec) + *E*(PB)
⟨*E*(tot)⟩	−4561.0	1.6	−4551.2	2.0	−9.8	*E*(gas) + *E*(PB) + *E*(nonpolar)
⟨salt: 0.1 M⟩	−28.7	0.0	−29.6	0.0	0.9	linear salt contribution
⟨salt: 0.1 M⟩	−31.6	0.0	−39.4	0.0	7.8	nonlinear salt contribution
⟨salt: 1.0 M⟩	−34.5	0.1	−42.9	0.1	8.4	nonlinear salt contribution

[a,b] See footnotes to Table 1.

Table 3. Results for d(CGCGAATTCGCG)$_2$

	"BD3"		"AD3"			
energy	mean[a]	σ[b]	mean[a]	σ[b]	(B − A)	notes
⟨*E*(elec)⟩	388.3	7.0	608.8	5.5	−220.5	Coulomb energy
⟨*E*(vdW)⟩	−207.3	1.0	−209.8	1.0	2.5	van der Waals energy
⟨*E*(int)⟩	1035.8	1.8	1056.2	1.8	−20.4	internal energy
⟨*E*(gas)⟩	1216.8	7.3	1455.2	5.5	−238.4	total vacuum energy
⟨*E*(nonpolar)⟩	26.7	0.0	26.3	0.0	0.4	nonpolar solvation energy
⟨*E*(PB)⟩	−6472.1	6.6	−6697.0	5.3	224.9	Poisson Boltzmann
⟨*E*(GB)⟩	−6470.5	6.6	−6699.1	5.3	228.6	generalized Born
⟨*E*(elec_tot)⟩	−6083.8	1.2	−6088.2	1.1	4.4	*E*(elec) + *E*(PB)
⟨*E*(tot)⟩	−5228.6	1.6	−5215.6	1.4	−13.0	*E*(gas) + *E*(PB) + *E*(nonpolar)
⟨salt: 0.1 M⟩	−38.6	0.0	−40.7	0.0	2.1	linear salt contribution
⟨salt: 0.1 M⟩	−43.6	0.1	−48.9	0.1	5.3	nonlinear salt contribution
⟨salt: 1.0 M⟩	−53.6	0.1	−59.7	0.2	6.1	nonlinear salt contribution

[a,b] See footnotes to Table 1.

Table 4. Results for NP-d(CGCGAATTCGCG)$_2$

	"BNP"		"ANP"			
energy	mean[a]	σ[b]	mean[a]	σ[b]	(B − A)	notes
⟨*E*(elec)⟩	−1658.8	4.9	−1222.6	19.9	−436.2	Coulomb energy
⟨*E*(vdW)⟩	−187.6	1.1	−189.2	0.9	1.6	van der Waals energy
⟨*E*(int)⟩	1142.9	2.3	1114.2	2.1	28.7	internal energy
⟨*E*(gas)⟩	−703.4	4.6	−297.7	1.9	−405.7	total vacuum energy
⟨*E*(nonpolar)⟩	26.3	0.0	26.1	0.0	0.2	nonpolar solvation energy
⟨*E*(PB)⟩	−6541.8	4.3	−6959.3	18.5	417.5	Poisson Boltzmann
⟨*E*(GB)⟩	−6507.9	4.3	−6927.9	18.9	420.0	generalized Born
⟨*E*(elec_tot)⟩	−8200.5	2.2	−8182.0	2.0	−18.5	*E*(elec) + *E*(PB)
⟨*E*(tot)⟩	−7218.9	1.6	−7230.9	1.5	12.0	*E*(gas) + *E*(PB) + *E*(nonpolar)
⟨salt: 0.1 M⟩	−36.9	0.0	−39.7	0.1	2.8	linear salt contribution
⟨salt: 0.1 M⟩	−38.8	0.0	−53.8	0.5	15.0	nonlinear salt contribution
⟨salt: 1.0 M⟩	−52.2	0.1	−65.1	0.5	12.2	nonlinear salt contribution

[a,b] See footnotes to Table 1.

the phosphate groups are arranged more in a line, and the distance between them (across the major groove and along the backbone) is smaller than for the B-form. Hence the gas-phase electrostatic values, ⟨*E*(elec)⟩ in the tables, are greater in the A-form by 200−300 kcal/mol for DNA and RNA and by a larger amount for the phosphoramidate-modified DNA. This force-field number excludes 1−2 and 1−3 interactions and divides 1−4 electrostatic interactions by 1.2,[22] but the excluded interactions should be roughly independent of conformation.

To a large (but not complete) extent, the effect of electrostatic solvation is to screen charge−charge interactions, so that most of the gas-phase electrostatic energy that favors the B-form is canceled by corresponding terms favoring A in the ⟨*E*(PB)⟩ numbers. The total electrostatic energy (at zero added salt) is given as ⟨E(elec_tot)⟩. Since solvation screens much of the gas-phase electrostatic interactions, the fluctuations in *E*(elec_tot) are substantially smaller than those of *E*(elec) or *E*(PB) individually. This behavior has been noted before.[15,16] The total electrostatic interaction favors the B-form helix by small amounts for the first two DNA sequences and A by a small amount for the dodecamer sequence of Table 3. For the RNA and NP-modified DNA system, electrostatics favors the B-form by a larger amount. This illustrates the fact that the "A-form" and "B-form" labels used here are not rigid entities but are equilibrated (meta)stable energy basins whose details differ from one system to another.

Tables 1−5 also show results from generalized Born calculations, ⟨*E*(GB)⟩, which can be compared to the ⟨*E*(PB)⟩ numbers. In each case, the B−A difference from the GB model is within 5 kcal/mol of that determined from the much more computationally demanding PB model. This correspondence holds not only for the means but also for the individual conformers as well. Figure 1 plots the individual solvation energies computed from both theories for the 100 snapshots for the B-form DNA

Table 5. Results for r(CCAACGUUGG)$_2$

	"BR"		"AR"			
energy	mean[a]	σ^b	mean[a]	σ^b	(B − A)	notes
⟨*E*(elec)⟩	−333.4	3.7	−66.5	5.0	−266.9	Coulomb energy
⟨*E*(vdW)⟩	−149.4	1.1	−168.1	0.9	18.7	van der Waals energy
⟨*E*(int)⟩	944.0	1.8	926.4	1.9	17.6	internal energy
⟨*E*(gas)⟩	461.3	4.1	691.7	4.8	−230.4	total vacuum energy
⟨*E*(nonpolar)⟩	22.7	0.0	22.6	0.0	0.1	nonpolar solvation energy
⟨*E*(PB)⟩	−4796.3	3.4	−5036.5	4.4	240.2	Poisson Boltzmann
⟨*E*(GB)⟩	−4787.4	3.3	−5029.6	4.5	242.2	generalized Born
⟨*E*(elec_tot)⟩	−5129.7	1.3	−5103.0	1.1	−26.7	*E*(elec) + *E*(PB)
⟨*E*(tot)⟩	−4312.4	1.7	−4322.2	1.8	9.8	*E*(gas) + *E*(PB) + *E*(nonpolar)
⟨salt: 0.1 M⟩	−29.0	0.0	−30.4	0.0	1.4	linear salt contribution
⟨salt: 0.1 M⟩	−32.1	0.0	−35.5	0.1	3.4	nonlinear salt contribution
⟨salt: 1.0 M⟩	−40.1	0.0	−44.0	0.1	3.9	nonlinear salt contribution

[a,b] See footnotes to Table 1.

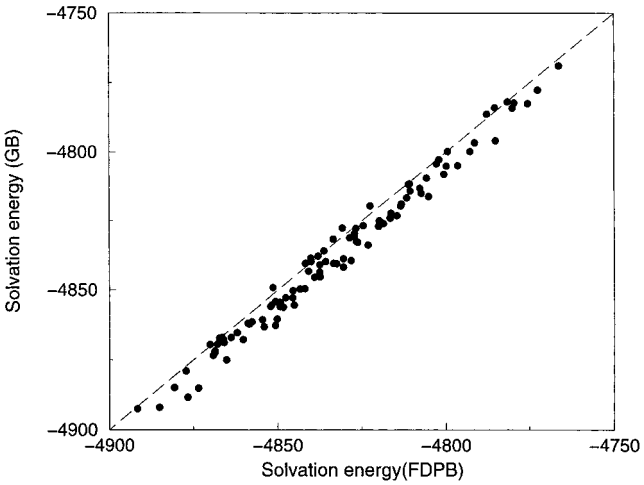

Figure 1. GB and PB solvation energies for the BD1 conformers from Table 1. Energies are in kcal/mol.

reported in Table 1. It is clear that there is a good correspondence between the two methods. There are a variety of variants of generalized Born models, and the particular one used here is described in the Methods; a more detailed discussion of these results, along with a comparison to other approaches, will be presented elsewhere.

2.2. Effects of Added Salt. The contributions of added salt are known to be important for DNA structure and dynamics in general and to the A−B helix transition in particular.[23] For example, the d(ACCCGCGGGT)$_2$ sequence of Table 2 can be driven to A-form helices through the addition of hexaamminecobalt(III) ions.[24] Other DNA sequences (that lack the poly-dC·poly-dG motif) appear to be more difficult to drive toward A-form.[25] The proper treatment of added salt is a complex problem,[26−28] and the values given in the tables, for the linear and nonlinear Poisson−Boltzmann model, should be viewed as estimates of the energetics involved. Since added salt mainly screens electrostatic interactions, it should favor conformers with higher gas-phase electrostatic energies, in this case the A-form helices. This is borne out by the salt contributions shown in Tables 1−5, which are reported as differences between the Poisson results at zero added salt and the results for 0.1 or 1.0 M monovalent added salt. The B−A differences are always positive, i.e. added salt always favors the A-form more than the B-form.

At the Debye−Huckel (linearized PB) level, 0.1 M salt has a small relative effect for these oligonucleotides of 10−12 base pairs: the stabilization of A vs B ranges from 0.9 to 2.8 kcal/mol. These differences are considerably larger for the nonlinear PB model, ranging from 3.4 to 7.8 kcal/mol. Values for the much higher salt concentration of 1.0 M stabilize the A-form by 10−15% more than at 0.1 M, suggesting that Debye screening is already effective even at fairly low added salt.

2.3. Sugar Pucker Preferences. A second main difference between A- and B-form helices resides in sugar pucker, which is in the N (north) pseudorotation range for A and in S (south) for B.[23] In force field terms, energetic preferences between these two sugar conformers appears to reside primarily in electronic interactions that stabilize gauche geometries for O−C−C−O torsions.[29,30] Figures 2 and 3 illustrate these preferences by plotting mean energies for some torsion angle terms for the sequences of Tables 1, 4, and 5. Figure 2 considers the O4′−C1′−C2′−O2′ interaction, which is present in RNA but not DNA. For DNA (with H2″ in the place of O2′) there is little energetic difference for this torsion angle between the N and S sugars, but for RNA, most sugars (except at the helix ends) are about 2 kcal/mol more stable in the A-form N conformer than in the B-form S configuration. The sum of the B−A torsion energy differences in Figure 2 is 3 kcal/mol for DNA and 41 kcal/mol for RNA. This preference is then reflected in the ⟨*E*(int)⟩ values in Tables 1 and 5: the B-helix is favored by 7.0 kcal/mol for the deoxy helix (Table 1) but disfavored by 17.6 kcal/mol in the RNA helix (Table 5).

A second contribution to the force-field dissection of sugar-pucker energetics comes from the O4′−C4′−C3′−O3′ torsion shown in Figure 3. This angle is the "mirror image" of the O4′−C1′−C2′−O2′ torsion discussed above, favoring S sugar puckers over N. Since it is present in both DNA and RNA, one might not expect it contribute to an explanation of why RNA favors A-form helices and DNA favors the B-form. However, the "A" helices found in the ethanol water simulation used here actually have several S sugars at various times during the trajectory,[31] so that this torsion actually contributes in different ways to the A−B difference for DNA compared to

(23) Saenger, W. *Principles of nucleic acid structure*; Springer-Verlag: New York, 1984.
(24) Robinson, H.; Wang, A. H. J. *Nucleic Acids Res.* **1996**, *24*, 676−682.
(25) Peticolas, W. L.; Wang, Y.; Thomas, G. A. *Proc. Natl. Acad. Sci. U.S.A.* **1988**, *85*, 2579−2583.
(26) Anderson, C. F.; Record, M. T., Jr. *Annu. Rev. Phys. Chem.* **1995**, *46*, 657−700.
(27) Bloomfield, V. A. *Curr. Opin. Struct. Biol.* **1996**, *6*, 334−341.
(28) Chen, S. W.; Honig, B. *J. Phys. Chem. B* **1997**, *101*, 9113−9118.
(29) Olson, W. J. *J. Am. Chem. Soc.* **1982**, *104*, 278−286.
(30) Cheatham, T. E., III; Kollman, P. A. In *Structure, Motion, Interactions and Expression of Biological Macromolecules*; Sarma, R. H., Sarma, M. H., Eds.; Adenine Press: Albany, NY, 1998; pp 99−116.
(31) Cheatham, T. E., III; Crowley, M. F.; Kollman, P. A. *Proc. Natl. Acad. Sci. U.S.A.* **1997**, *94*, 9626.

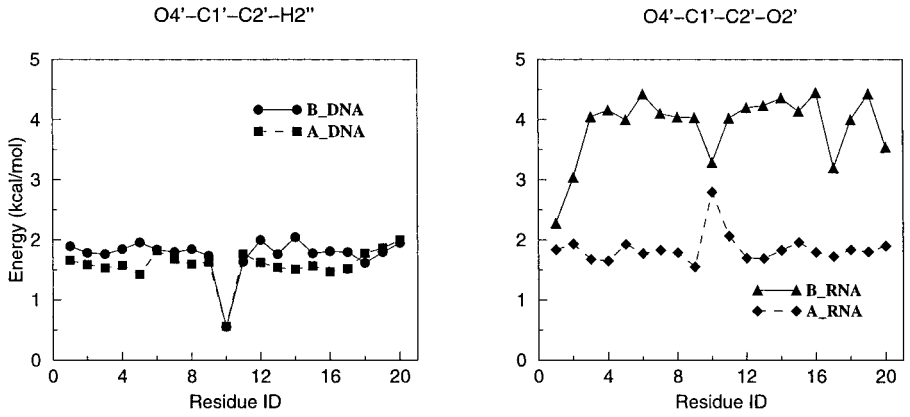

Figure 2. Mean internal (bond-angle-dihedral) energies for O4′−C1′−C2′−O2′(H2″) calculated for the MD trajectories of the A- and B-forms of RNA and DNA decamer simulations shown in Tables 1 and 5.

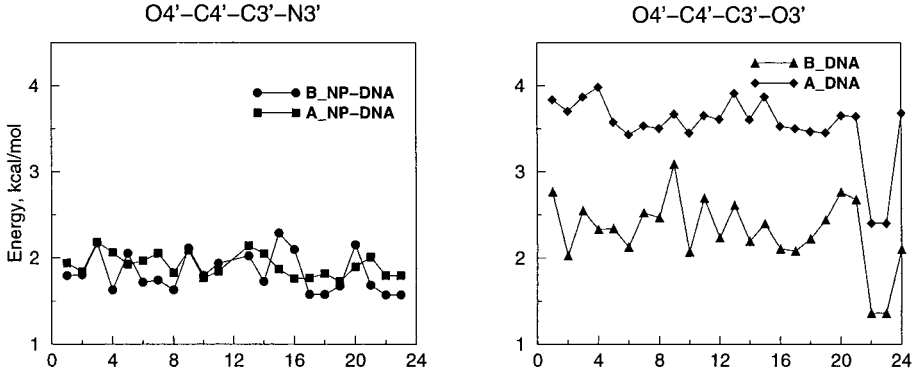

Figure 3. Mean internal (bond-angle-dihedral) energies for O4′−C4′−C3′−O3′(N3′) calculated for the MD trajectories of the A- and B-forms of the unmodified and NP-modified dodecamers of Tables 3 and 4.

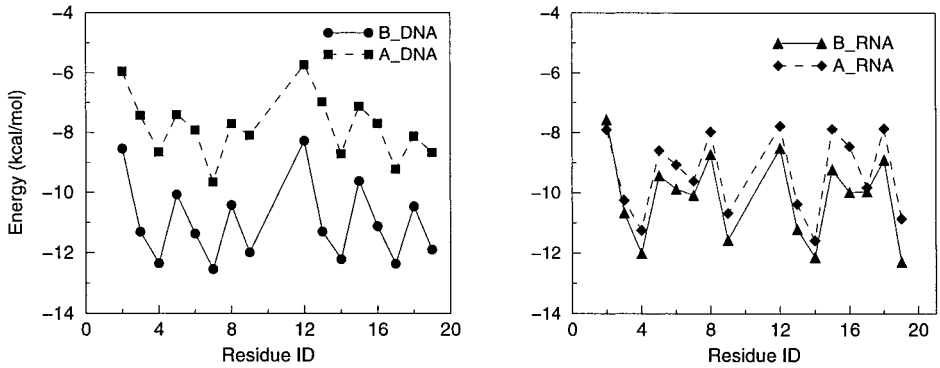

Figure 4. van der Waals stacking energies for the DNA and RNA forms calculated from the decamer MD simulations of Tables 1 and 5.

RNA. Similar arguments can be used to explain the sugar-pucker preferences in the phosphoramidate-modified DNA. Here the O4′−C4′−C3′−O3′ torsion in DNA is replaced with O4′−C4′−C3′−N3′, which has no V_2 term to represent the gauche preference, at least in the force field parametrization used here,[12] which rationalized the lack of a V_2 term based on NMR data for nucleosides with H, NH, and OH at the 3′ position. This removes the preference for S sugars that is present in DNA, leading to nearly equal energies for N and S sugar puckers with the modified backbone and hence to a relative stabilization of A-form helices compared to B. The relative stabilization of A-helices from this term alone (26 kcal/mol, the sum of the differences in Figure 3) is about the same as the total extra stabilization of the A-helix in the modified compared to unmodified system (compare Tables 3 and 4).

2.4. van der Waals Interactions with the 2′ OH Group. We calculated van der Waals interaction energies for each of the 2′-hydroxyl group from the AR and BR trajectories of Table 5. Average energies for the two forms of RNA showed only small differences for the individual 2′ OH groups between A- and B-helices. However, since there are 20 such groups in the decamer, the total van der Waals difference favors the A-form by about 19 kcal/mol. Much of this comes from unfavorable steric interactions of the 2′ OH with its own base in the B-conformation. Hence, a simple steric difficulty of putting a ribose base into the B-form is supported by these calculations.

2.5. Stacking Energies. Base-stacking energies are known to have an important effect on DNA conformation and stability. Figure 4 shows intrastrand van der Waals interaction energies, i.e. for each base, the Lennard-Jones energy with neighboring bases along the same strand. This term systematically favors B-helices over the A-form, but by a larger amount for DNA than for RNA: these stacking energies favor the B-form helix by 51 kcal/mol for DNA and by 12 kcal/mol for RNA. As Figure 4 shows, the main effect is from less favorable stacking interactions in the A-form DNA than in the other three forms.

2.6. Solute Entropy. The solute entropy contribution to the free energy of the A → B transition is one of the most difficult terms to estimate in our model. We have used a simple harmonic model described in the Methods. The entropy estimated in this way is 1696.4 cal/(mol·K) for B−RNA and 1706.1 cal/(mol·K) for A-RNA. The A-form has slightly greater flexibility, with a free energy difference of 3.0 kcal/mol at 300 K. For DNA with the same sequence, the B-DNA entropy is 1757.8 cal/(mol·K) and the A-DNA result is 1759.5 cal/(mol·K), corresponding to a free energy favoring the A-form of 0.5 kcal/mol at 300 K. These are only a rough estimates, since the harmonic model, which is roughly valid at low temperatures, should fail when the solute dynamics involve significant motion from one conformational well to another.[32,33] In addition to relatively small sugar fluctuations (say in going from a B_I to a B_{II} conformation, or with minor populations of "N" sugars in B-form helices), contributions from base-fraying, especially at the ends of these short helices, could make significant contributions to the solute entropy. It is not known how such effects will depend on the type of helix; the current model effectively assumes that they are the same in the A- and B-forms and hence do not contribute to relative free energy differences. Given the limitations of the harmonic model used here, it is probably best to conclude merely that the solute entropy differences between A- and B-form helices are small.

It would clearly be of interest to have better ways to estimate solute entropy, but there can be difficulties when the dynamics at room-temperature jump between basins.[33] Even within the linear (quasi-harmonic) approximation,[32] relative entropies of A- and B-form helices are sensitive to the number of snapshots used and portion of trajectory analyzed (results not shown). Jayaram et al. have recently reported quasiharmonic calculations on $d(CGCGAATTCGCG)_2$ (the sequence of Table 3) that favor the B-form helices by a small amount.[34] It is clear that increased attention to this point will be required if the methods used here are to be applied to a wider variety of problems, especially where one set of conformers is substantially floppier than others.

3. Discussion

We have presented estimates of the structure-dependent free energies of five DNA and RNA helices, using a combination of the internal energies derived from all-atom liquid-phase simulations and solvation free energies derived from continuum solvent models. One very attractive feature of this model is that there are no cutoffs for long-range interactions: we include all solute−solute electrostatic interactions, and the boundary conditions of the continuum model the correct long-range behavior for the solvent polarization terms. Hence, in contrast to most force-field analyses of biomolecular energetics, the total energies of different conformations should reflect genuine differences in conformational stability. To the extent that this works, it removes the usual requirement to construct an explicit pathway between conformations to compute free energy differences.

A second attractive feature of the continuum solvent model is that it implicitly provides averages over the water and counterion degrees of freedom, removing an onerous requirement of more detailed, explicit solvent calculations. Averaging over counterion degrees of freedom can be particularly important, since individual ions are fairly mobile and yet have strong electrostatic interactions with the sugar−phosphate backbone. This means that explicit simulations need to carry out extensive averaging to obtain mean interaction energies, making more attractive a continuum model that treats mobile ions in terms of continuous distributions. The drawback, of course, is that this model of solvation has quantitative limitations, ignores the molecular character of the solvent molecules, and is not easily extrapolated to other temperatures or solvents. The current results suggest that in many cases the continuum model is sufficiently realistic to be a useful adjunct to more detailed simulations.

The explicit-water simulations used here have just enough sodium counterions to neutralize the phosphates of the nucleic acid. In this sense, they probably correspond most closely to solution conditions with zero added salt, although the actual ionic strength due to the mobile counterions is about 0.15 M. Comparable simulations have recently been carried out with additional sodium and chloride counterions, corresponding to an ionic strength of about 1 M.[30] The structural parameters in simulated high- and low-salt conditions were very similar, supporting our practice here of using the same set of structural snapshots to analyze energetics for several values of ionic strength. Further studies of the structural and energetic consequences of added salt are certainly warranted.

Overall, our results are in good qualitative agreement with experiment. Specifically, all three DNA helices are predicted to favor the B-form. Further, the calculations appear to capture the DNA sequence dependence of the A−B free energy difference. It is known that polydG·polydC stretches tend to be more "A-philic" than alternating dC-dG stretches.[25] Consistent with this, we find that $d(CCAACGTTGG)_2$ favors the B-form of DNA by 21 kcal/mol whereas $d(ACCCGCGGGT)_2$ favors the B-form by only 10 kcal/mol. The latter sequence is known to convert to an A-helix in the presence of $Co(NH_3)_6^{3+}$. The calculations here show that even monovalent ions can nearly make the A- and B-forms equivalent for the sequence of Table 2. The reduced preference for a B-form helix in this latter sequence has contributions from internal energies, van der Waals repulsions, and electrostatics, although the first two are the largest.

Changing the 3′ oxygen to an NH group has been shown to stabilize A-DNA over the B-form experimentally and in MD simulations.[12,35] For example, in contrast to ordinary DNA (which undergoes a spontaneous A → B transition in about 0.5 ns in MD simulations), the phosphoramidate-modified form takes a similar amount of time to undergo the reverse B → A transition. The present calculations are consistent with this difference: DNA with sequence $d(CGCGAATTCGCG)_2$ (Table 3) favors B over A by 13 kcal/mol, whereas the corresponding modified form favors A by 12 kcal/mol. Here, the loss of the V_2 anomeric term for the O4′−C4′−C3′−O3′ interaction when NH is substituted for O3′ is a large contributor to the shift in equilibrium.

In comparing DNA to a corresponding RNA sequence, the calculations show DNA favoring the B-helix by 21 kcal/mol and RNA favoring A by 10 kcal/mol. The van der Waals and internal energies both contribute to this change because the 2′ OH group is crowded in a B-form helix, and the presence of both O4′−C1′−C2′−O2′ and O4′−C4′−C3′−O3′ anomeric effects in RNA drives the preference of ribose sugars more to the C3′-endo form characteristic of A-helices. Interestingly, the

(32) Karplus, M.; Kushick, J. N. *Macromolecules* **1981**, *14*, 325−332.
(33) Garca, A. E.; Soumpasis, D. M.; Jovin, T. M. *Biophys J.* **1994**, *66*, 1742−1755.
(34) Jayaram, B.; Sprous, D.; Young, M. A.; Beveridge, D. L. *Molecular thermodynamics of the conformational stability of A and B forms of DNA in solution*, 1998, submitted for publication.
(35) Tereshko, V.; Gryaznov, S.; Egli, M. *J. Am. Chem. Soc.* **1998**, in press.

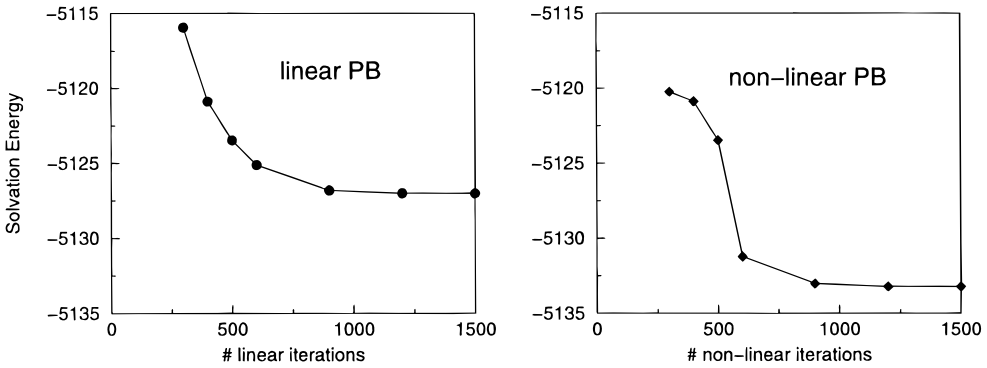

Figure 5. Delphi-II solvation energy for a BD1 conformer in the presence of 0.1 M 1:1 added salt as a function of the number of iterations: left panel, linear PB model; right panel, nonlinear PB iterations following 300 linear interations.

total electrostatic interactions favor B over A by a greater amount in RNA than in DNA (compare Tables 1 and 5).

Since the A-form helices always have less favorable phosphate−phosphate electrostatic interactions, the effect of salt is to screen these unfavorable interactions and hence to stabilize the A-form relative to B. The Poisson−Boltzmann model used here ignores ion−ion correlations (which would allow ions to approach each other more closely) and finite-size effects (which tend to keep ions apart). To a certain extent these terms cancel each other, but the salt effects shown in the tables should still be considered mainly as guides to the expected behavior. The results show that A-form helices are stabilized by 2−8 kcal/mol at 0.1 M added monovalent salt, with the nonlinear PB model giving a greater A−B difference than the linear model. The A−B difference appears to saturate at fairly low added salt concentration, so that results for 1.0 M added salt are not much different than those for 0.1 M.

In the current model, nonelectrostatic contributions to solvation free energies are represented by a surface-area-dependent term. This has little effect on the transitions considered here, since the solvent-accessible surface area is nearly the same in the two forms, differing by about 40 Å^2 for the sequence in Table 1, for example. Even if a larger proportionality constant were to be used to connect surface areas to free energies, this contribution would still be small, although it does consistently favor the A-form helices over B.

Very recently, Jayaram et al. have reported an energy analysis of the A- and B-forms of d(CGCGAATTCGCG)$_2$ that is similar in many ways to the results reported here.[34] They also took snapshots from explicit-solvent molecular dynamics simulations and added results from a generalized Born model to gas-phase force field energies to estimate relative free energies in solution. Consistent with the results reported here, these authors find the B-form helix to be more stable in water; they also created a continuum model for ethanol/water solvation, in which the A-helix was more stable. Although there are detailed differences in methodology (particularly in the way counterion electrostatic effects are incorporated into the model), the general results support the notion that a continuum solvation analysis can be a robust method to analyze conformational energetics in nucleic acid duplexes.

We are continuing to explore the performance of this model; results for RNA hairpins and hairpin−duplex conversions will be reported elsewhere. It should be emphasized that our model in no way eliminates the need for an accurate force field. A basic conclusion from this and previous studies[14−20] is that solutes (described by molecular mechanics) respond to solvation by a continuum model in very nearly the same way they respond to an explicit description of solvent using the TIP3P water model. The results reported here depend on a consistent use of the same solute force field in the simulations as in the energy analysis. Our use of the term "A-form" and "B-form" helix reflects what the Cornell et al. force field predicts for these structures, on average. Nevertheless, the results here should make it more straightforward to evaluate new force fields and simulations and point the way to an analysis that may provide insight into a wide variety of conformational problems in nucleic acids.

4. Theory and Methods

4.1. Simulations Examined. The structures considered here were taken from published molecular dynamics simulations that have been carried out in a consistent fashion using the Amber molecular modeling programs.[36] Details are given in the paragraphs below, but in general, all of the simulations used the Cornell et al. all-atom force field[22] (in the parm94.dat file of the Amber code) and the TIP3P model for water.[37] All simulations approximated long-range electrostatic interactions with the particle−mesh Ewald method (PME) procedure,[38,39] using a cubic B-spline interpolation and a 10^{-5} tolerance set for the direct space sum cutoff. This general procedure has been shown to provide a good account of many aspects of nucleic acid duplex structures.[5] The simulations examined in this study are described in the following paragraphs; in each case, the original papers should be consulted for further details and descriptions of the average structures.

(a) d(CCAACGTTGG)$_2$. For this decamer duplex, unrestrained dynamics simulations starting from either idealized A- or B-form structures converge on a nanosecond time scale to a single averaged structure in reasonably good agreement with experimental data.[40] For the "BD1" set (Table 1), we took 100 snapshots at 10-ps intervals starting at 0.4 ns of a trajectory that began from the idealized B-structure. The A-form simulation ("AD1" in Table 1) was initiated from a canonical A-form helix and simulated in an 85% ethanol environment,[31] where the A-form helix remains stable without any artificial constraints. Again, 100 structures at 10-ps intervals were selected starting 2 ns into the trajectory.

(b) d(ACCCGCGGGT)$_2$. The A-form simulation of this sequence ("AD2" in Table 2) was simulated with four hexaamminecobalt(III) ions and six Na^+ ions in water. Hexaamminecobalt(III) is known experimentally to stabilize A-form helices,[24] and simulations starting from both A- and B-form DNA converge to a common A-like structure.[10] We used the 100 snapshots at 10-ps intervals from the period beginning at 1 ns. The B-form simulation of this sequence ("BD2" in

(36) Pearlman, D. A.; Case, D. A.; Caldwell, J. W.; Ross, W. S.; Cheatham, T. E., III; DeBolt, S.; Ferguson, D.; Seibel, G.; Kollman, P. *Comput. Phys. Commun.* **1995**, *91*, 1−41.

(37) Jorgensen, W. L. *J. Chem. Phys.* **1982**, *77*, 4156.

(38) Essmann, U.; Perera, L.; Berkowitz, M. L.; Darden, T.; Lee, H.; Pedersen, L. G. *J. Chem. Phys.* **1995**, *103*, 8577−8593.

(39) Darden, T.; York, D.; Pedersen, L. *J. Chem. Phys.* **1993**, *98*, 10089−10092.

(40) Cheatham, T. E., III; Kollman, P. A. *J. Mol. Biol.* **1996**, *259*, 434−444.

Table 2) was taken from a simulation of this sequence in water with a neutralizing number of Na^+ counterions. The simulation started from a canonical A-form helix and underwent a spontaneous A → B transition during the first nanosecond, after which it stayed near the B-form. We selected 100 snapshots at 10-ps intervals starting at 1.92 ns.

(c) d(CGCGAATTCGCG)$_2$. These simulations ("BD3" and "AD3" in Table 3) were initiated from the canonical B- and A-forms geometries of this sequence, respectively. These simulations, performed in the presence of explicit water and neutralizing counterions, showed that the B-form geometry is the more stable form. To simulate the A-form structure the sugar pucker was constrained to the C3′-endo conformation by a 30 kcal/(mol·rad^2) harmonic constraint on the C1′−C2′−C3′−C4′ torsion to its canonical value. The 100 B-form snapshots began directly after the equilibration period; 100 A-form snapshots were selected at 5-ps intervals after 0.5 ns of simulation.

(d) (CCAACGUUGG)$_2$. These simulations ("BR" and "AR" in Table 4) started from the canonical B- and A-forms geometries of this sequence, respectively. These simulations showed that the RNA duplexes adopt (meta)stable A-form and a B-form helices on a nanosecond time scale.[4] A total of 100 snapshots of each were taken at 10-ps intervals beginning at 1.37 ns for the B-form and 1.03 ns for the A-form.

(e) NP-d(CGCGAATTCGCG)$_2$. The modification replaces the O3′ of a deoxy sugar with NH, maintaining the charge on the phosphate backbone, but changing torsional preferences as discussed in the Results. These simulations ("BNP" and "ANP" in Table 4) were initiated from the canonical B- and A-form geometries, respectively.[12] For the A-form simulation, we used the "NH-out" trajectory[12] and selected 100 snapshots at 15-ps intervals following the equilibration period. The simulation initiated from the B-form conformation in the absence of any constraints adopted an A-like structure within 500 ps. To maintain a B-form-like structure, the C1′−C2′−C3′−C4′ torsion was constrained to the region 322−332° by harmonic potentials outside this region with a force constant of 30 kcal/(mol·rad^2). We selected 100 snapshots at 4-ps intervals following the equilibration period. This simulation is also of the "NH-out" variety.

In total we analyzed 1000 conformational snapshots, 100 from each of five B-form simulations and five A-form simulations. The "gas-phase" energy of the nucleic acid solute (with no counterions or solvent) was computed from the Cornell et al. force field used in the simulations[22] with no cutoff for nonbonded interactions. Averages of these energies, divided into electrostatic, van der Waals, and internal (bond, angle, and dihedral) energies, are given in Tables 1−5. Estimates of solvation energies were made as described in the following paragraphs.

4.2. Electrostatic Solvation Free Energies. Nucleic acid oligomers are highly charged molecules, and a key aspect of their solvation energies (especially for differences between A- and B-forms) lies in their electrostatic interaction with solvent. The continuum model used here posits a low dielectric solute with embedded charges surrounded by a high dielectric continuum solvent. The dielectric boundary is taken as the molecular surface defined by a 1.4 Å probe sphere and by spheres centered on each atom with radii taken from the PARSE parameter set[41] (H = 1.0, C = 1.7, N = 1.5, O = 1.4), with a value of 2.0 for phosphorus. Partial charges on the solute atoms are taken from the Cornell et al. force field,[22] in order to be consistent with the energetics of the explicit simulations we are analyzing. The solute is assigned a dielectric of 1, consistent with our use of a nonpolarizable molecular mechanics force field; in this model, the solute response to charge fluctuations is estimated through explicit averaging of conformations, rather than by use of an interior dielectric greater than unity. The solvent dielectric is set to 80. Both Poisson−Boltzmann and generalized Born models were used to evaluate the electrostatic component to the solvation free energy.

4.2.1. Poisson Boltzmann (PB) Approach. In the PB model, calculations were based on the finite difference solution to the Poisson equation:[21,42,43]

$$\nabla\epsilon(r)\nabla\phi(r) + 4\pi\rho(r) = 0 \qquad (1)$$

where $\phi(r)$ is the electrostatic potential, $\epsilon(r)$ is the position dependent dielectric function, and $\rho(r)$ is the charge density due to the solute. For systems of the size discussed here, it is not trivial to obtain accurate and stable results. In the Delphi-II program used here, the solute with its associated charges is mapped on to a grid and the electrostatic potentials due to the presence of a dielectric continuum solvent are determined by solving the Poisson equation. We used a grid spacing of 0.25 Å with a cubic lattice whose linear dimensions were about 50% larger than the longest dimension of the solute; this yielded lattices of 185^3, 197^3, 241^3, 251^3, and 185^3 for the systems reported in Tables 1−5, respectively. Potentials at the boundaries of the finite-difference lattice were set to sum of the Debye−Huckel potentials:[44]

$$\phi = \sum_i q_i \frac{\exp(-\kappa r)}{\epsilon r} \qquad (2)$$

Here ϕ is the potential estimate at a given lattice boundary point, q_i is an atomic partial charge, r is the distance from the lattice boundary to the charge, κ is the Debye screening parameter, and ϵ is the solvent dielectric constant.

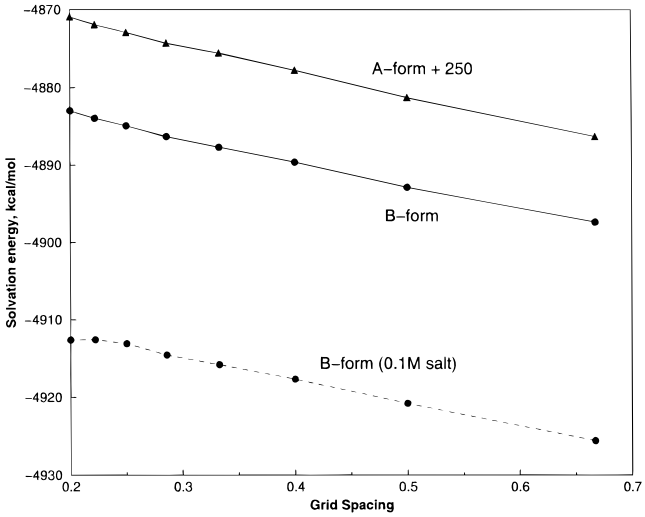

Figure 6. Delphi-II solvation energies for a BD1 and an AD1 conformer as a function of grid spacing. All calculations used a cubic grid with 201 points per side. Results for the A-form have been shifted upward by 250 kcal/mol to fit on the graph.

Numerical Considerations. The choice of lattice size is a tradeoff between higher resolution with finer grid spacings versus increased memory and time requirements. Figure 5 illustrates the convergence of the over-relaxation scheme in Delphi: for both the linear and nonlinear PB model at 0.1 M added salt, nearly 1000 iterations are required to obtain converged results. Convergence behavior is a strong function of the size of the grid, with results such as those in Figure 5 being typical of what we see for a 200^3 grid in either the Delphi or MEAD[45] finite-difference programs. We used 1500 finite difference iterations for the results reported here, although a smaller number probably would have been sufficient. For both Delphi and MEAD, the default convergence criteria are often too loose to converge problems of this size.

Calculated solvation energies also depend to a significant degree on the grid resolution chosen. Figure 6 illustrates the convergence with grid spacing for three sample duplexes. The absolute solvation energy dependence is significant: reducing the grid spacing from 0.5 to 0.2 Å changes the solvation energy by about 10 kcal/mol for these problems. However, as has been noted before,[44] the dependence is quite smooth,

(41) Sitkoff, D.; Sharp, K. A.; Honig, B. *J. Phys. Chem.* **1994**, *98*, 1978−1988.
(42) Warwicker, J.; Watson, H. C. *J. Mol. Biol.* **1982**, *157*, 671−679.
(43) Sharp, K. A.; Honig, B. *Annu. Rev. Biophys. Biophys. Chem.* **1990**, *19*, 301−332.
(44) Gilson, M. K.; Sharp, K. A.; Honig, B. H. *J. Comput. Chem.* **1987**, *9*, 327−335.
(45) Bashford, D.; Gerwert, K. *J. Mol. Biol.* **1992**, *224*, 473−486.

and relative energies of different conformers, or estimates of the effect of added salt, are reasonably independent of grid resolution over a wide range, as is illustrated in Figure 6. The results reported here used a grid spacing of 0.25 Å; as with the iteration count, it is clear that a larger spacing could be used in future studies, with a corresponding increase in computational efficiency.

Salt Effects. To study the effect of added salt on DNA/RNA structures, both linear and nonlinear solutions to the PB equations have been computed.[46] Salt terms reported in Tables 1−5 are differences from the corresponding zero-salt terms labeled $\langle E(\mathrm{PB})\rangle$. Unlike the total solvation free energy, which has a range of more than 100 kcal/mol even for snapshots taken from the same trajectory (see Figure 1), the computed salt dependence is much more constant, so that the statistical uncertainties reported in the tables are quite small. This suggests that, in future studies, many fewer snapshots could be used to estimate salt effects in this manner.

4.2.2. Generalized Born (GB) Approach. In the second approach, the electrostatics are modeled by the generalized Born model:[47] term:

$$\nabla G_{\mathrm{Born}}^{\mathrm{GB}} = \left(1 - \frac{1}{\epsilon}\right)\sum_{ij}\frac{q_i q_j}{(r_{ij}^{\,2} + \alpha_{ij}^{\,2}\exp(-D_{ij}))^{0.5}} \qquad (3)$$

where $\alpha_{ij} = (\alpha_i\alpha_j)^{0.5}$, $D_{ij} = r_{ij}^2/2\alpha_{ij}^2$, and the double sum runs over all pairs of atoms, including terms where $i = j$. α_i is the effective Born radius of atom i, and the exponential is used to force the $\Delta G_{\mathrm{Born}}^{\mathrm{GB}}$ term to approximate the dielectric part of the Coulomb's law rapidly as the atoms move beyond the contact distance of their Born radii.

The effective Born radius (α) for a simple spherical solute where the charge resides at the center of this sphere (as in a model for a metal ion) can be close to the van der Waals radius of the solute. However, for more complex solutes, the effective Born radius (α_i) depends on the positions and volumes of all other solute atoms because they displace the solvent-like dielectric medium. Physically the Born radius of an atom is not so much a radius as it is the average distance from the charge on the atom to its dielectric boundary. Several recent studies have reported fast analytical methods to calculate approximate Born radii for complex molecule shapes,[48−50] and in this study, we adopt the approximate pairwise method to calculate the "effective" Born radius as described by Hawkins et al.[49] with parameters developed in the *tinker* molecular modeling package.[51] A fuller discussion of the performance of GB methods for nucleic acid modeling will be given elsewhere; the present results illustrate that the GB model can often be an effective and efficient alternative to PB calculations for problems in conformational energetics.

4.3. Nonpolar Contributions to the Solvation Energy. The nonpolar contribution to solvation, i.e. the free energy of solvation of the "discharged" molecule in which all the atom-centered partial charges are set to zero, was modeled as a term that is dependent on the solvent-accessible surface area of the molecule. This term is represented as $\gamma\mathrm{SA} + b$, where SA is the surface area of the solute, γ is taken to be 0.00542 kcal/Å^2, and b is 0.92 kcal/mol.[41] The solvent-accessible surface area was evaluated using the algorithm of Sanner.[52] Although the total contribution of this nonpolar term is significant, the exposed surface area changes little with helix form, so that there is little effect on the A vs B energy difference from this term.

4.4. Estimates of Solute Entropy. The continuum solvation models discussed above provide estimates of the free energies of solvation, i.e., they implicitly incorporate averages over the solvent degrees of freedom. To complete the estimates of the free energy differences between A- and B-form helices, we must also estimate the entropy components arising from solute degrees of freedom. This in general can be quite a difficult problem, especially if the magnitude of solute fluctuations is significantly different from one conformational well to another. To investigate this, we have carried out normal mode calculations on A- and B-forms of d(CCAACGTTGG)$_2$ and (CCAACGTTGG)$_2$ (cf. Tables 1 and 5). This requires minimum energy structures of the solute alone that are similar to the structures seen in solvated simulations. To obtain these, we carried out minimizations in the absence of solvent, but with a dielectric constant of 4r (where r is the interatomic distance in Å) to mimic solvent screening. Conjugate gradient and Newton−Raphson minimizations were carried out, starting from idealized helices, until the root-mean-square of the elements of the gradient vector was less than 10^{-4} kcal/(mol·Å). These minimizations cause the structure to move about 2 Å from the starting positions, so care should be taken in interpreting the results, but the qualitative features are expected to be reliable.

Acknowledgment. This work was supported by NIH Grants RR-12255 (to D.A.C.) and CA-25644 (to P.A.K.). We thank Don Bashford and Paul Beroza for helpful comments and David Beveridge for communicating results prior to publication. We thank the Pittsburgh Computer Center Metacenter for computational resources.

JA981844+

(46) Sharp, K. A.; Honig, B. *J. Phys. Chem.* **1990**, *94*, 7684−7692.
(47) Still, W. C.; Tempczyk, A.; Hawley, R. C.; Hendrickson, T. *J. Am. Chem. Soc.* **1990**, *112*, 6127−6129.
(48) Qiu, D.; Shenkin, P. S.; Hollinger, F. P.; Still, W. C. *J. Phys. Chem. A* **1997**, *101*, 3005−3014.
(49) Hawkins, G. D.; Cramer, C. J.; Truhlar, D. G. *Chem. Phys. Lett.* **1995**, *246*, 122−129.
(50) Hawkins, G. D.; Cramer, C. J.; Truhlar, D. G. *J. Phys. Chem.* **1996**, *100*, 19824−19839.
(51) Dudek, M. J.; Ramnarayan, K.; Ponder, J. W. *J. Comput. Chem.* **1998**, *19*, 548. See also http://dasher.wustl.edu/tinker.
(52) Sanner, M. F.; Olson, A. J.; Spehner, J.-C. *Biopolymers* **1996**, *38*, 305−320.